



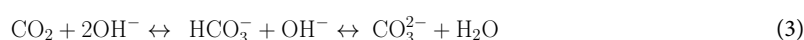
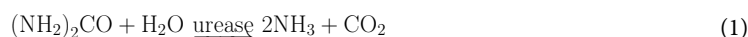
# OPEN Evaluation of encapsulated *Bacillus subtilis* bio-mortars for use under acidic conditions

Chanachai Thongchom<sup>1</sup>, Tunyaboon Laemthong<sup>2</sup>✉, Panisa Sangkeaw<sup>1</sup>,  
Nattapong Yamasamit<sup>1</sup> & Suraparb Keawsawasvong<sup>1</sup>

This research aimed to examine the effects of an acidic environment on the mechanical properties and durability of bio-mortar (BM) encapsulated with *Bacillus subtilis* bacteria, in comparison to normal mortar (NM). The results at 28 days indicated that both 3% and 6% HCl significantly increased the compressive strength of the BM by 25% and 50%, respectively, compared with that of the NM. However, when 11% HCl was introduced, the compressive strength of the BM decreased to 50% lower than that of the NM. Furthermore, the water absorption rate of the BM was 33% lower than that of the NM. The mass loss for both 3% and 6% HCl was comparable, whereas at 11% HCl, BM experienced a mass loss that was 68% greater than that of NM. These findings suggest that with 3% and 6% HCl, the microbially induced calcium carbonate precipitation (MICP) process effectively generated  $\text{CaCO}_3$ , which filled the pores and enhanced the structural integrity of the BM, leading to improved compressive strength and durability. Conversely, at 11% HCl, the MICP benefits in BM were diminished due to adverse environmental conditions that negatively affected the bacterial cells, highlighting the limitations of the HCl concentration for optimizing MICP efficiency in mortar.

**Keywords** *Bacillus subtilis*, Concrete, Mortar, Mechanical properties, Microbially induced calcium carbonate precipitation (MICP)

One of the current issues that often occurs in mortar and concrete work is crack formation caused by improper hardening, exposure to abrupt environmental changes or shrinkage. Concrete fissures increase permeability, which shortens the service life of steel reinforcement by accelerating corrosion<sup>1</sup>. Procedures such as grouting and epoxy filling are used to repair cracks<sup>2,3</sup>. However, these procedures require continuous efficient maintenance, causing a rise in energy usage and, moreover, some possible release of toxicity to the environment<sup>4</sup>. Bio-mortar is thus introduced to address this problem. The crack-closing ability of bio-mortar decreases over time because of the diminished effectiveness of microbially induced calcium carbonate precipitation (MICP)<sup>5</sup>. Factors such as reduced bacterial activity, nutrient depletion, and environmental conditions can impact the efficiency of MICP, ultimately affecting the ability of bio-mortar to heal cracks and maintain structural integrity<sup>6</sup>. MICP requires bacteria that produce urease to react with nutrients and urea to form bio-mediated calcium carbonate ( $\text{CaCO}_3$ ), as described in Eqs. (1–4)<sup>7</sup>. The crystallization of  $\text{CaCO}_3$  or calcite was mainly a product of a urea hydrolysis reaction via bacterial urease. MICP occurs at the bacterial cell surface.



Thus, bio-mortar and concrete are considered eco-friendly materials that contribute to reducing maintenance costs, energy consumption, and possible greenhouse gas (GHG) emissions<sup>8</sup> by autonomously repairing cracks through MICP processes<sup>6</sup>. These materials increase the durability and longevity of structures, minimizing

<sup>1</sup>Research Unit in Structural and Foundation Engineering, Department of Civil Engineering, Faculty of Engineering, Thammasat School of Engineering, Thammasat University, Pathum Thani 12120, Thailand. <sup>2</sup>Department of Chemical Engineering, Faculty of Engineering, Thammasat School of Engineering, Thammasat University, Pathum Thani 12120, Thailand. ✉email: ltunyabo@engr.tu.ac.th

the need for frequent repairs and lowering the overall environmental impact. Members of *Bacillus* sp. are extensively used in bio-mortar and concrete research due to their rapid growth rate and high survival rate<sup>9</sup>. When the concrete hardens, an oxidation reaction occurs, resulting in a high pH (up to 12.5)<sup>10</sup>. Owing to their spore-forming ability, for example, *Bacillus subtilis* and *Bacillus sphaericus* are able to survive extremely alkaline conditions and other possibly extreme environments<sup>11,12</sup>. *B. subtilis* is a gram-positive, nonpathogenic facultative anaerobe that produces catalase and other enzymes to hydrolyze nutrients for survival. *B. subtilis* exhibits urease activity and  $\text{CaCO}_3$  precipitation ability<sup>13,14</sup>. The optimal pH conditions for *B. subtilis* were found to be approximately 4.8–9.1<sup>15</sup>. Urea hydrolysis increases the pH, but its product ( $\text{CO}_2$ ) acts as a buffer to maintain the pH<sup>16,17</sup>. *B. sphaericus* are mesophilic bacteria that produce endospores that are resistant to heat, chemicals, and ultraviolet light<sup>18</sup>. Microencapsulation techniques are used for self-healing cement because of their ability to provide efficient protection from external environmental conditions, such as heat, light, and humidity<sup>19,20</sup>. Bacteria are trapped inside microcapsules, which consist of a shell or coating such as gum Arabic, sodium alginate, or phospholipids. Once the microcapsules are exposed to a selected factor, such as pH, increased temperature or pressure, or hydrolytic enzymes, trapped bacteria are released<sup>21,22</sup>. Here, we examine the effects of acidic environments on the mechanical properties of bio-mortars that incorporate encapsulated *B. subtilis*. By analyzing how these bio-mortars behave under acidic conditions, this study aims to assess their durability and structural integrity, particularly focusing on the influence of acid exposure on compressive strength and overall performance.

## Materials and methods

### Bacterial strains and reagents

*B. subtilis* strains were obtained via the procedures described in<sup>13</sup>. All chemicals were purchased from Kemaus AR. grade, and the culture medium was obtained from BD Difco unless otherwise specified.

### Bacterial cell culture and microencapsulation

*B. subtilis* was initially cultured in tryptic soy broth (TSB) supplemented with 0.212%  $\text{NaHCO}_3$  and 1% urea. The cells were grown at 30 °C with 100 rpm agitation. After 7 days, the cultures were incubated at 80 °C for 10 min and immediately quenched in an ice bath for 5 min. The cultures were transferred to fresh TSB medium supplemented with  $\text{NaHCO}_3$  and urea and then incubated at 30 °C with 100 rpm agitation for 2 days. The incubated cell cultures were centrifuged at 8,000 rpm at 4 °C to remove the supernatant. The cell pellets were collected and washed three times with 0.1% NaCl-containing peptone water. The cell pellets were kept in 1% glycerol at 4 °C. The prepared bacterial cell pellets were resuspended in 2% sodium alginate until they reached  $10^8$  CFU/mL. The cell suspension was frozen at -40 °C for 24 h, followed by freeze-drying at -40 °C. Freeze-dried cells were minced and kept at 0 °C until further use (see Fig. 1).

### Bio-mortar preparation

Normal mortar (NM) and bio-mortar (BM) were prepared according to ASTM C109, as described in Table 1. For BM, encapsulated *B. subtilis* cell pellets were resuspended in  $\text{CaCl}_2$  solution for 30 min at room temperature (RT) to induce MICP prior to the mixing steps. Mortar was prepared by mixing all the ingredients at  $140 \pm 5$  rpm for 30 s followed by mixing at  $285 \pm 10$  rpm for 30 s. The mixture was agitated for 90 s and shaken at  $285 \pm 10$  rpm for another 60 s. The mixture was poured into a cube mold (5 cm × 5 cm × 5 cm) to prepare the specimens.

### Characterization and testing of mortar

A compressive strength test was performed for both the NM and BM specimens according to ASTM C109 by dividing the specimens into 4 groups: the NM group after the specimens were incubated at RT for 1, 3, 7, 14, and

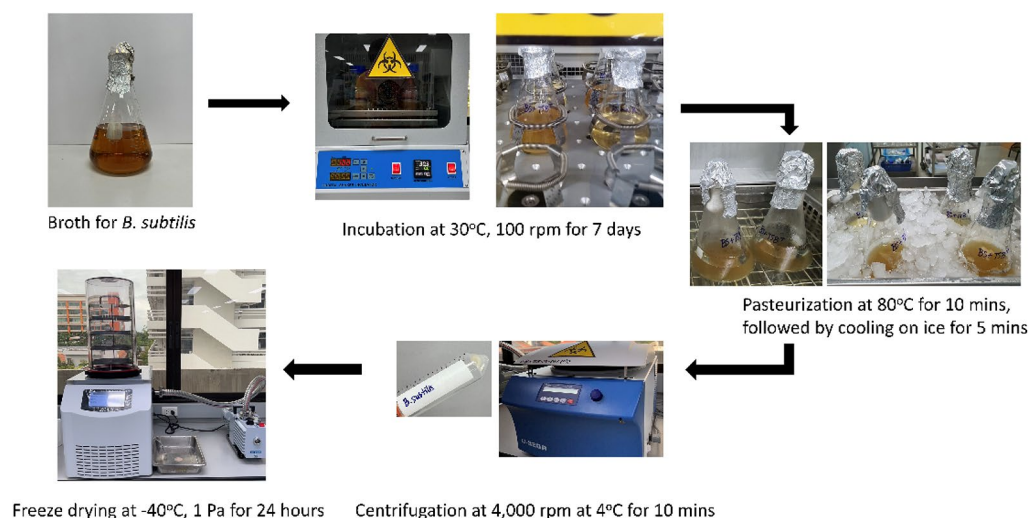


**Fig. 1.** Process of microencapsulation.

Ingredient	Weight (g)	
	(Normal mortar) NM	(Bio-mortar) BM
Portland cement type 1	826.7	826.7
Water	400.9	400.9
Sand	1136.7	1136.7
Encapsulated bacterial cells	–	16.5

**Table 1.** Composition of the NMs and BMs used in this study.

28 days; the BM group after the specimens were incubated at RT for 1, 3, 5, 7, 14, and 28 days; the Normal Acidified Compressive Strength (NAC) group after soaking the NM specimens in 3%, 6%, and 11% HCl for 7, 14, and 28 days; and the Bacterial Acidified Compressive Strength (BAC) group after the BM specimens were soaked in 3%, 6%, and 11% HCl for 7, 14, and 28 days. The pH values of the 3%, 6% and 11% HCl solutions were 0.39, 0.01 and –0.18, respectively. The compressive strength values (f) were calculated from Eq. 5.

$$f = \frac{P}{A} \times 10 \tag{5}$$

where P is the ultimate load of the specimens and A is the cross-sectional area.

**Water absorption testing of mortar**

The mortar specimens were dried at 110 ± 5 °C for 24 h and cooled at RT for 4 h. The dry weight ( $W_d$ ) of the specimens were recorded. The specimens were submerged in RT water for 24 h, and their saturated weight ( $W_s$ ) was recorded. The experiment was conducted for 1, 2, 3, 4, 5, 7, 14, and 28 days. The water absorption percentages of the mortar were calculated via the following equation:

$$\% \text{Absorption} = \frac{W_s - W_d}{W_d} \times 100 \tag{6}$$

**Weight change evaluation of the mortar**

All mortar specimens were incubated at 110 °C to remove internal moisture and were left for at least 4 h to cool to RT. The initial weights of the specimens were recorded. Afterwards, the specimens were soaked in 3% HCl for 7, 14, or 28 days. After soaking, the specimens were left at RT for 2 days. The specimens were incubated at 110 °C for 24 h and left at RT for 24 h. The final weight of each specimen ( $W_f$ ) was recorded. The experiments were performed at least in triplicate.

**Microstructural analysis**

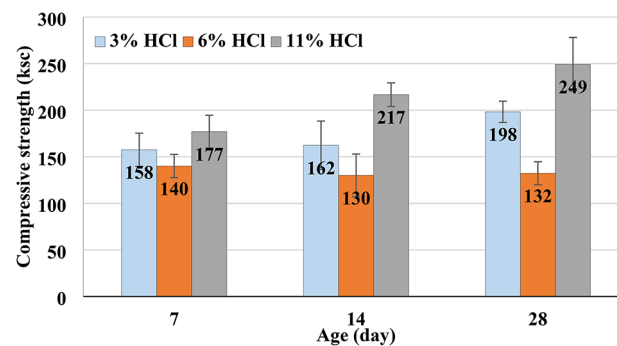
The surface of the sample and embedded microencapsulated bacteria was visualized using FE-SEM (SU8030 Hitachi Scanning Electron Microscopy (SEM)).

**Results and discussion**  
**Compressive strength test**

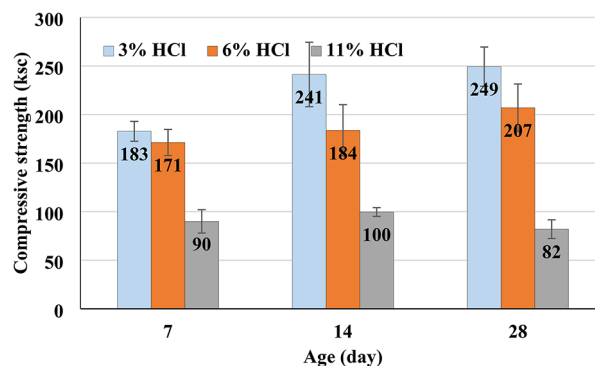
As one of the important mortar properties, a compressive strength test was conducted for both the NM and BM samples after acidic corrosion for 7, 14, and 28 days. In a 3% HCl solution, the BM samples exhibited a 30–50% greater compressive strength than did the NM samples after 7 and 14 days of incubation and a 25% greater compressive strength after 28 days of incubation. In a 6% HCl solution, the BM also exhibited approximately 20%, 40%, and 50% greater compressive strength than those NM after 7, 14, and 28 days of incubation, respectively. The increase in the compressive strength of the BM was a result of *B. subtilis* MICP on the outer layer of the samples. However, in an 11% HCl solution, the compressive strength of the BM drastically decreased by more than 50% compared with that of the NM. The significant reduction in compressive strength observed in BM exposed to an 11% HCl solution may have been caused by the detrimental effects of high acidity on mortar stability (Fig. 2). The heightened acidity impedes bacterial vitality, and the process of  $\text{CaCO}_3$  precipitation, even under acidic conditions, corrodes the internal structure of the cement matrix, potentially resulting in reduced compressive strength<sup>23</sup>. Under mildly acidic conditions, the porous outer layer was sealed with precipitated  $\text{CaCO}_3$ , and the inside was protected from harsh conditions, providing more time for *B. subtilis* to undergo MICP and fill the porous structure. Moreover, NM lacks of MICP ability, exposing the inner layer of mortar to acidic conditions and leading to a lower compressive strength. However, in an 11% HCl solution, the acidity exceeded the range of the optimal pH at which *B. subtilis* can grow. These conditions inhibited *B. subtilis* growth and urease activity, leading to material degradation over time.

**Water absorption**

As depicted in Fig. 3, within periods of 1, 3, and 7 days, the water absorption rates of the BM samples were notably lower than those of the NM samples, with reductions of 8.7%, 22.1%, and 22.6%, respectively. Similarly, as the mortar was incubated for 14 and 28 days, the trend persisted, with the BM group consistently exhibiting lower water absorption. Specifically, the absorption in the NM group decreased by 32.84% and 32.95%, respectively. The decrease in water absorption is attributed to the MICP process, which prompts the precipitation of calcium



(a) Normal mortar (NM)



(b) Bio-mortar (BM)

**Fig. 2.** Analysis of the compressive strength of NM and BM after incubation in various concentrations of HCl solution. Under mildly acidic conditions, such as 3% and 6% HCl, the compressive strength of the BM increased after incubation. However, in 11% HCl, cell growth is inhibited by excessive acidic conditions, leading to the loss of MICP ability of *B. subtilis* and eventually to mortar degradation.

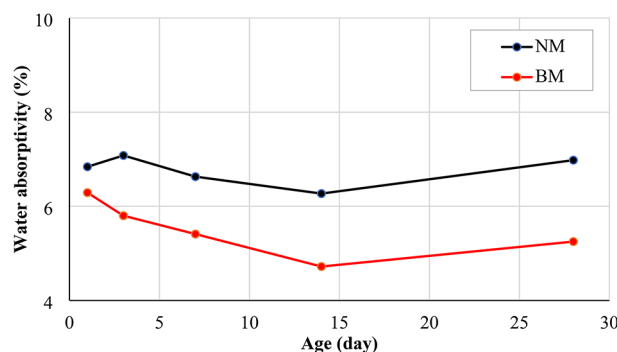
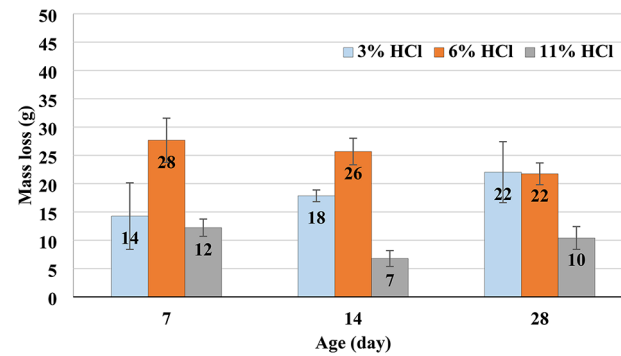


**Fig. 3.** Water absorptivity comparison between normal mortar (NM) and bio-mortar (BM) after 1, 3, 7, 14, and 28 days of incubation. NM and BM lose their water absorptivity after incubation.

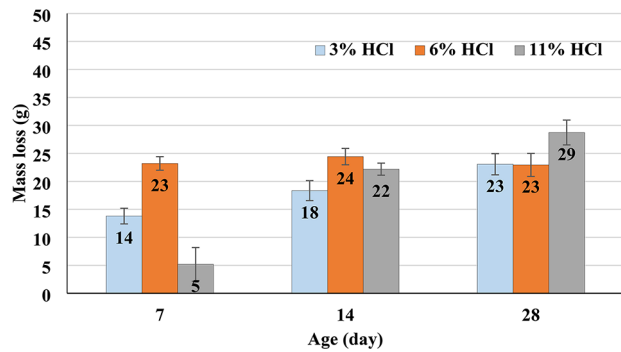
carbonate ( $\text{CaCO}_3$ ), thus aiding in the filling of minute cracks within the naturally porous cement matrix of the mortar. Consequently, this process effectively reduces porosity, thereby limiting water absorption within the mortar by decreasing the number of interconnected pores, and the mortar becomes less permeable to water, which enhances its durability and resistance to moisture-related damage<sup>13</sup>.

### Acidic resistance property

To mimic mildly acidic environments, the samples were mixed with various concentrations of HCl, and the mass loss relative to the dry weight of the samples was determined (Figs. 4 and 5). After 7 days of incubation in a 3% HCl solution, the mass loss of BM was 31.3% less than that of NM. After 14 days of sample age, it was observed that at 3% HCl, NM and BM showed comparable mass loss values. In the case of 6% HCl, NM displayed a greater mass loss than BM, measuring 7.69%. However, with 11% HCl, the results contrasted with those of 6% HCl, as BM experienced a higher mass loss than NM, reaching 68.16%. However, the mass loss of

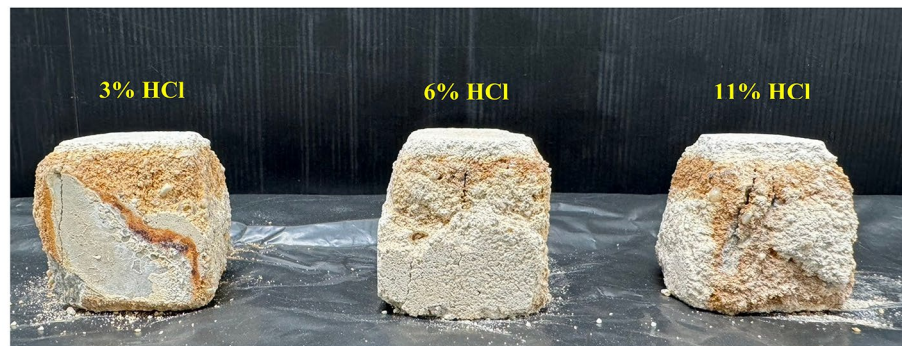


(a) Normal mortar (NM)

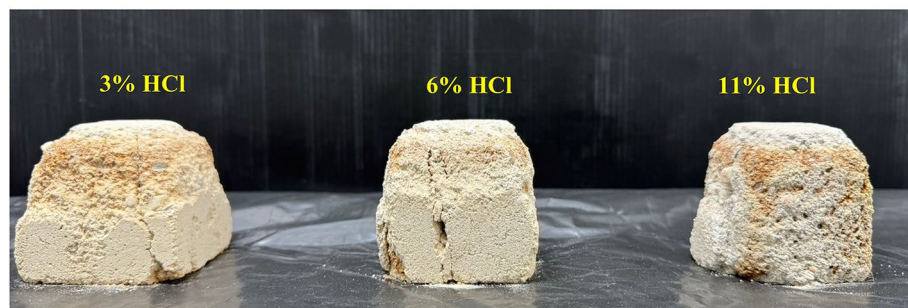


(b) Bio-mortar (BM)

**Fig. 4.** The mass loss of the samples showing the acid resistance of the BM under mildly acidic conditions. Higher mass losses indicate lower acid resistance.



(a) Normal mortar (NM)



(b) Bio-mortar (BM)

**Fig. 5.** NM and BM after incubation in different concentrations of HCl for 28 days.



the BM increased by 37.72% compared with that of the NM after 28 days of incubation. For 6% HCl, the mass loss of the BM was 36.47% greater than that of the NM after 7 days of incubation and approximately 5% less than that of the NM after 14 days of incubation. However, after 28 days of incubation, the mass loss of the BM was 9.57% greater than that of the NM. A similar trend was observed for both samples after they were placed in 11% HCl. After 7 days of incubation, the mass loss of the BM was 15.91% less than that of the NM, but the mass loss of the BM after 14 days was 35.29% greater than that of the NM. However, the mass loss of the BM was 13.93% greater than that of the NM after 28 days of incubation. Bio-mortars utilize MICP, where bacteria facilitate the precipitation of calcium carbonate ( $\text{CaCO}_3$ ). This initial calcite formation creates a protective layer that shields the underlying mortar matrix from acid attack. In the early stages, this protective layer remains intact, resulting in reduced mass loss compared to conventional mortars, which lack such biological protection. The reaction between HCl and the components of bio-mortar is not instantaneous. The presence of microbial byproducts and initial calcite slows the rate at which HCl interacts with the mortar matrix. This gradual reaction allows for temporary preservation of mass until the protective layers are compromised<sup>24</sup>.

After the protective layer has deteriorated, this becomes evident after 14 days. The overall mass loss of BM was greater than that of NM due to the degradation of bacterial culture media in the outer surface layer of the samples caused by exposure to an acidic environment. However, neither the NM nor the BM could resist the high concentration of HCl (11%) used in this study since all the samples swelled and started to disintegrate after incubation. Moreover, the highly acidic environment was not suitable for *B. subtilis*, which can grow in a slightly acidic environment. Moreover, the cells were not trapped inside the mortar because of the disintegration of the structure.

### Investigation of *B. subtilis* viability and surface structure

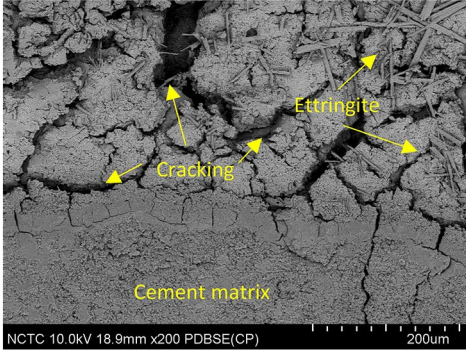
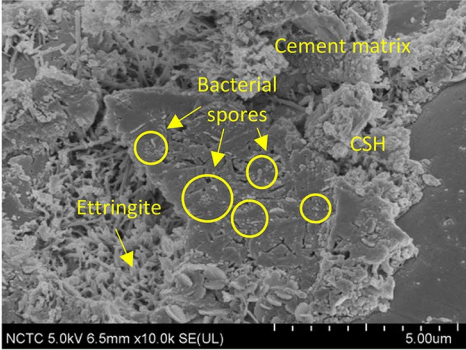
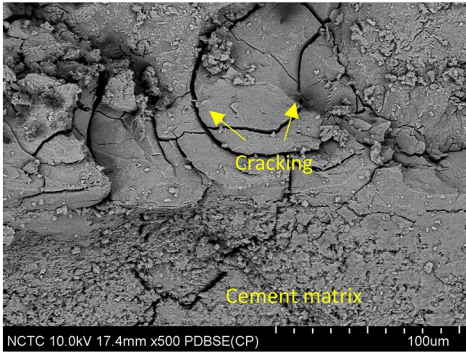
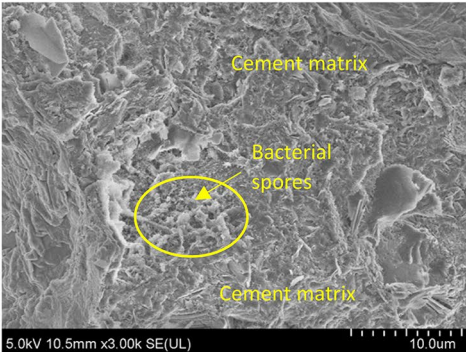
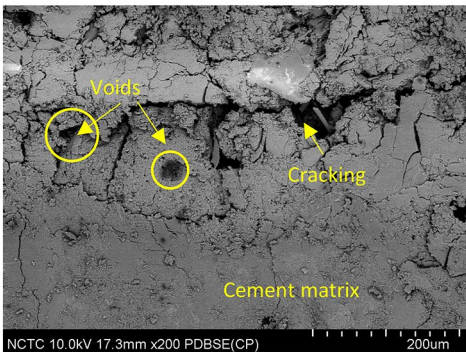
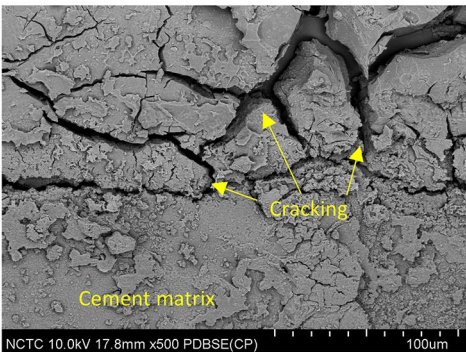
Scanning electron microscopy (SEM) images of the samples were analyzed to inspect the viability of *B. subtilis*. The samples were incubated in 3%, 6%, and 11% HCl solutions. SEM images revealed that *B. subtilis*, as rod-shaped cells, spread within the BM samples. *B. subtilis* was found in clusters of numerous cells, as shown in Fig. 6. More fine particles, presumably sand, were found across the NM image. Moreover, in those incubated in 11% HCl solution, the SEM images of both the NM and BM were similar. No cells were found in the samples. The results confirmed that most cells were able to survive in mildly acidic conditions, such as 3% and 6% HCl. Unlike in the samples incubated in an 11% HCl solution, no cells were observed in the samples since the cells were killed due to improper pH conditions. In addition, SEM images of the NMs revealed the presence of cement hydration products such as CSH and the formation of ettringites within the cement matrix. Moreover, cracks and voids were observed within the matrix. Moreover, the BM contained small, clustered *B. subtilis* spores embedded within the cement matrix (see Fig. 6).

The microstructure of the bio-mortars after incubation in hydrochloric acid was analyzed for the weight% composition of the elements in the mortar by an energy dispersive X-ray spectrometer (EDS). The percentages of calcium (Ca), carbon (C), and silicon (Si) in the specimens after they were incubated in 3%, 6%, and 11% hydrochloric acid and in water for 28 days were compared between the NM and BM samples. The percentage by weight based on the observed mass loss after incubation of the samples is presented in Table 2. The mass loss indicates the corrosive effect of the acid on the mortar.

To conduct this analysis, both NMs and BMs were examined using an EDS system to assess and verify the chemical component peaks within them. As depicted in Fig. 7, all mortar samples exhibited a high calcium peak. However, this phenomenon is particularly prominent in BMs. Typically, mortar primarily consists of calcium as its main component. However, in the BM treatment, the calcium content was notably greater than that in the NM treatment. This disparity was attributed to the ability of the mortar to utilize the calcium present in the cement hydration product during water incubation, leading to the precipitation of  $\text{CaCO}_3$ . The increase in the amount of calcium suggested the accumulation of calcium carbonate crystals within the matrix. Nevertheless, elevated concentrations of HCl acid resulted in a reduction in elemental carbon and calcium. This reduction is likely due to the interaction of HCl with  $\text{CaCO}_3$ , leading to the following chemical reaction:  $\text{CaCO}_3 + 2\text{HCl} \rightarrow \text{CaCl}_2 + \text{CO}_2 + \text{H}_2\text{O}$ . This reaction neutralizes the acid while generating byproducts, consequently diminishing the proportions of carbon and calcium<sup>25,26</sup>. Moreover, the observation that non-hydraulic silicates remain unchanged further supports the conclusion that there is no significant change in the aggregate fraction. If this attack had occurred, the compounds within the aggregate would have dissolved in solution, with the lost silicates likely originating from the components and hydration products of the cement<sup>27</sup>.

### Conclusions

While bio-mortars have been extensively studied using several bacterial strains, there is always a need to improve bio-mortars to overcome some limitations. Mechanical and durability properties such as compressive strength and acid resistance are important for construction materials. Since bio-mortar, is considered an alternative way to be eco-friendly and to avoid maintenance costs over normal mortar, their properties need to be at least at the same level. Under normal conditions, it is clear that bio-mortars can potentially resolve crack problems<sup>14,28</sup>. Bio-mortars rely heavily on external factors such as curing processes, pH, and temperature. However, under some conditions, such as in acidic environments, bio-mortars are limited by biological constraints such as bacterial nutrients, growth factors, and strains. These factors compromised the mortar's properties and decreased its service life. As shown in this study, encapsulated *B. subtilis* induced MICP in mortar only in slightly acidic environments. At 28 days, the conclusions indicate that at 3% and 6% HCl, the compressive strength was higher in the BM than in NM by 25% and 50%, respectively. In contrast, at 11% HCl, BM exhibited lower compressive strength than NM by 50%, suggesting that selecting microorganisms capable of MICP formation in harsh environments would enhance the compressive strength properties of BM. BM had a lower water absorption rate than did NM by 33%, indicating that water absorption decreased over time because of the presence of closed

Condition	Normal mortar (NM)	Bio-mortar (BM)
3% HCl		
6% HCl		
11% HCl		

**Fig. 6.** Microstructural images of NMs and BMs after exposure to different acidic conditions.

pores. For mass loss, 3% and 6% HCl resulted in similar mass loss values. However, at 11% HCl, mass loss was more pronounced, with BM showing a greater mass loss value than NM at 68%.

Specimen	C (% by weight)	Si (% by weight)	Ca (% by weight)
HCl 3%			
NM	2.79	10.10	26.61
BM	4.67	20.70	31.02
HCl 6%			
NM	1.06	17.69	10.18
BM	3.14	13.18	27.18
HCl 11%			
NM	0.34	12.71	9.44
BM	2.28	8.56	23.75

**Table 2.** Percentage by weight of elements in NM and BM after incubation in different concentrations of HCl solution, as determined by EDS.

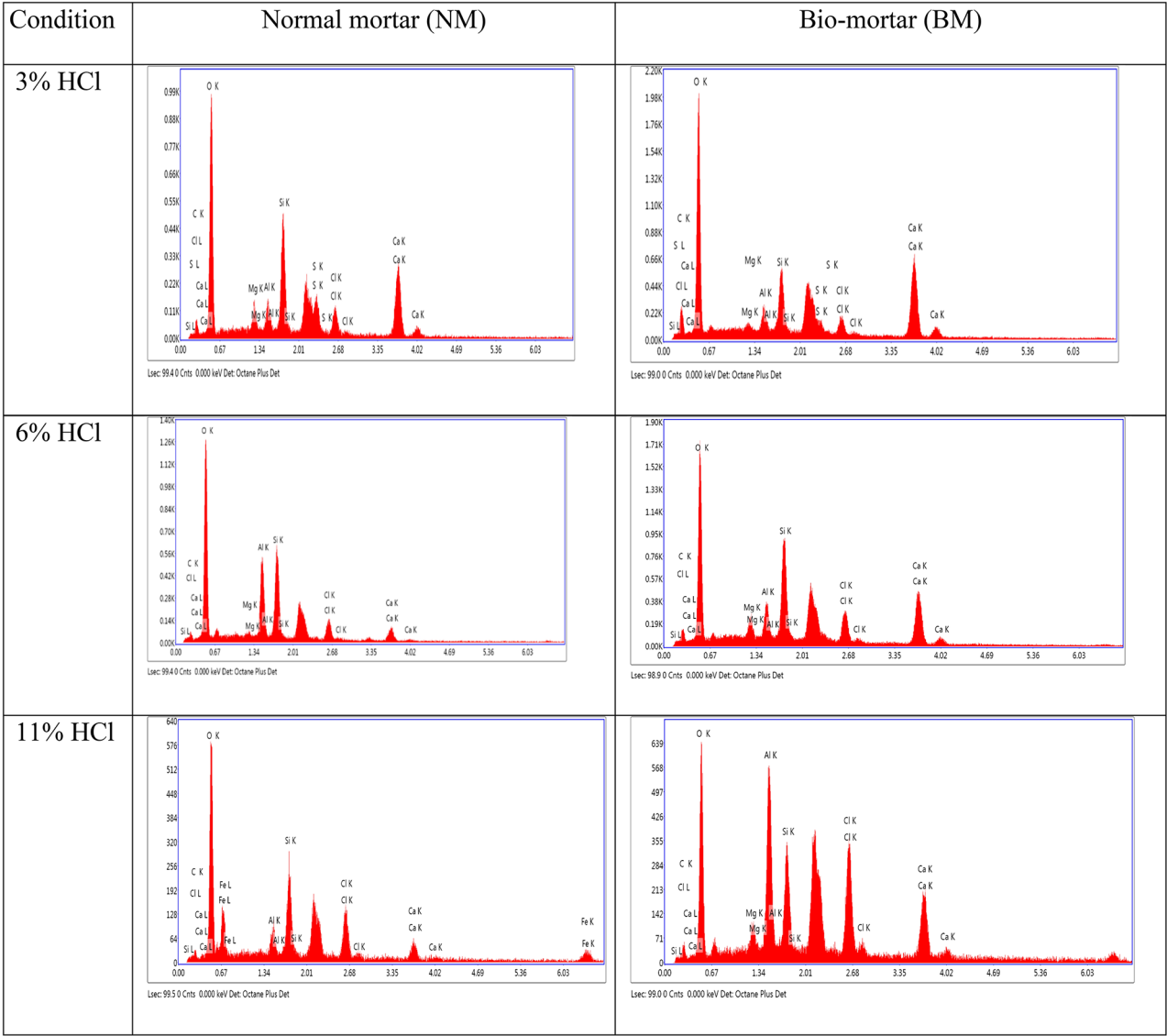


**Fig. 7.** Analysis of the chemical components of NM and BM under different acidic conditions.

**Data availability**

The datasets generated and analyzed during the current study are available from the corresponding author on reasonable request.



Received: 2 May 2024; Accepted: 22 October 2024

Published online: 29 October 2024

## References

1. Achal, V., Mukherjee, A. & Reddy, M. S. Microbial concrete: way to enhance the durability of building structures. *J. Mater. Civ. Eng.* **23**, 730–734 (2011).
2. Issa, C. A. & Debs, P. Experimental study of epoxy repairing of cracks in concrete. *Constr. Build. Mater.* **21**, 157–163 (2007).
3. Zhang, B. et al. Modified cement-sodium silicate material and grouting technology for repairing underground concrete structure cracks. *Arab. J. Geosci.* **12**, 1–10 (2019).
4. Bras, A., Gão, R., Lúcio, V. & Chastre, C. Development of an injectable grout for concrete repair and strengthening. *Cem. Concr. Compos.* **37**, 185–195 (2013).
5. Castro-Alonso, M. J. et al. 5 Microbially induced calcium carbonate precipitation (MICP) and its potential in bioconcrete: microbiological and molecular concepts. *Front. Mater.* **6**, 126 (2019).
6. Zhang, K. et al. Bin Shi. Microbial-induced carbonate precipitation (MICP) technology: a review on the fundamentals and engineering applications. *Environ. Earth Sci.* **82**, 229 (2023).
7. Jiang, N. J., Yoshioka, H., Yamamoto, K. & Soga, K. Ureolytic activities of a urease-producing bacterium and purified urease enzyme in the anoxic condition: implication for subseafloor sand production control by microbially induced carbonate precipitation (MICP). *Ecol. Eng.* **90**, 96–104 (2016).
8. Seifan, M., Samani, A. K. & Berenjian, A. Bioconcrete: next generation of self-healing concrete. *Appl. Microbiol. Biotechnol.* **100**, 2591–2602 (2016).
9. Mokhtar, N., Johari, M. A. M., Tajarudin, H. A., Al-Gheethi, A. A. & Algaifi, H. A. A sustainable enhancement of bio-cement using immobilised *Bacillus sphaericus*: optimization, microstructural properties, and techno-economic analysis for a cleaner production of bio-cementitious mortars. *J. Clean. Prod.* **318**, 128470 (2021).
10. Kovler, K., Roussel, N. & 10 Properties of fresh and hardened concrete. *Cem. Concr. Res.* **41**, 775–792 (2011).
11. Wang, J., Jonkers, H. M. & Boon, N. De Belie, N. *Bacillus sphaericus* LMG 22257 is physiologically suitable for self-healing concrete. *Appl. Microbiol. Biotechnol.* **101**, 5101–5114 (2017).
12. Fajardo-Cavazos, P. & Nicholson, W. *Bacillus* endospores isolated from granite: close molecular relationships to globally distributed *Bacillus* spp. from endolithic and extreme environments. *Appl. Environ. Microbiol.* **72**, 2856–2863 (2006).
13. Yamasmit, N. et al. Effect of *Bacillus subtilis* on mechanical and self-healing properties in mortar with different crack widths and curing conditions. *Sci. Rep.* **13**, 7844 (2023).
14. Mutitu, K. D. et al. Effects of biocementation on some properties of cement-based materials incorporating *Bacillus* species bacteria—a review. *J. Sustainable Cement-Based Mater.* **8**, 309–325 (2019).
15. Gauvry, E., Mathot, A. G., Couvert, O., Leguérinel, I. & Coroller, L. Effects of temperature, pH and water activity on the growth and the sporulation abilities of *Bacillus subtilis* BSB1. *Int. J. Food Microbiol.* **337**, 108915 (2021).
16. Zhu, X., Wang, J., De Belie, N. & Boon, N. Complementing urea hydrolysis and nitrate reduction for improved microbially induced calcium carbonate precipitation. *Appl. Microbiol. Biotechnol.* **103**, 8825–8838 (2019).
17. Wong, L. S. Microbial cementation of ureolytic bacteria from the genus *Bacillus*: a review of the bacterial application on cement-based materials for cleaner production. *J. Clean. Prod.* **93**, 5–17 (2015).
18. Dick, J. et al. Bio-deposition of a calcium carbonate layer on degraded limestone by *Bacillus* species. *Biodegradation*. **17**, 357–367 (2006).
19. Fahimzadeh, M., Diane Abeyratne, A., Mae, L. S., Singh, R. R. & Pasbakhsh, P. Biological self-healing of cement paste and mortar by non-ureolytic bacteria encapsulated in alginate hydrogel capsules. *Materials*. **13**, 3711 (2020).
20. Wang, J. et al. Application of modified-alginate encapsulated carbonate producing bacteria in concrete: a promising strategy for crack self-healing. *Front. Microbiol.* **6**, 1088 (2015).
21. Ali, M., Mukhtar, H. & Dufossé, L. Microbial calcite induction: a magic that fortifies and heals concrete. *Int. J. Environ. Sci.* **20**, 1113–1134 (2023).
22. Soda, P. R. K. et al. Performance assessment of sustainable biocement mortar incorporated with bacteria-encapsulated cement-coated alginate beads. *Constr. Build. Mater.* **411**, 134198 (2024).
23. Smitha, M. P., Suji, D., Shanthi, M. & Adesina, A. Application of bacterial biomass in biocementation process to enhance the mechanical and durability properties of concrete. *Clean. Mater.* **3**, 100050 (2022).
24. Chu, S. C. et al. Mohamad Ibrahim. Insights into the current trends in the utilization of bacteria for microbially induced calcium carbonate precipitation. *Materials*. **13**(21), 4993 (2020).
25. Schwantes-Cezario, N. et al. Effects of *Bacillus subtilis* biocementation on the mechanical properties of mortars. *Rev. IBRACON Estrut. Mater.* **12**, 31–38 (2019).
26. Scandifio, P. et al. Anti-erosive effect of calcium carbonate suspensions. *J. Clin. Exp. Dent.* **10**, e776 (2018).
27. Alvarez, J. et al. Methodology and validation of a hot hydrochloric acid attack for the characterization of ancient mortars. *Cem. Concr. Res.* **29**, 1061–1065 (1999).
28. Lu, C., Ge, H., Li, Z. & Zheng, Y. Effect evaluation of microbial mineralization for repairing load-induced crack in concrete with a cyclic injection-immersion process. *Case Stud. Constr. Mater.* **17**, e01702 (2022).

## Acknowledgements

This work was supported by the Faculty of Engineering Research Fund, Thammasat University, and was also supported by the Thailand Science Research and Innovation Fundamental Fund.

## Author contributions

C.T. conceptualized. All investigated. C.T., T.L., N.Y. validated. P.S. analyzed using software. C.T. and T.L. wrote the original manuscript. C.T., T.L., P.S. and S.K. reviewed the manuscript. C.T. and S.K. provided financial support for this study.

## Declarations

## Competing interests

The authors declare no competing interests.

## Additional information

**Correspondence** and requests for materials should be addressed to T.L.

**Reprints and permissions information** is available at [www.nature.com/reprints](http://www.nature.com/reprints).

**Publisher's note** Springer Nature remains neutral with regard to jurisdictional claims in published maps and institutional affiliations.

**Open Access** This article is licensed under a Creative Commons Attribution-NonCommercial-NoDerivatives 4.0 International License, which permits any non-commercial use, sharing, distribution and reproduction in any medium or format, as long as you give appropriate credit to the original author(s) and the source, provide a link to the Creative Commons licence, and indicate if you modified the licensed material. You do not have permission under this licence to share adapted material derived from this article or parts of it. The images or other third party material in this article are included in the article's Creative Commons licence, unless indicated otherwise in a credit line to the material. If material is not included in the article's Creative Commons licence and your intended use is not permitted by statutory regulation or exceeds the permitted use, you will need to obtain permission directly from the copyright holder. To view a copy of this licence, visit <http://creativecommons.org/licenses/by-nc-nd/4.0/>.

© The Author(s) 2024